Journal of Photochemistry & Photobiology, A: Chemistry 415 (2021) 113303

Contents lists available at ScienceDirect

Journal of Photochemistry & Photobiology, A: Chemistry

journal homepage: www.elsevier.com/locate/jphotochem

Carbazole-hydrazinobenzothiazole a selective *turn-on* fluorescent sensor for Hg^{2+}ions – Its protein binding and electrochemical application studies

Denzil Britto Christopher Leslee [a], Karuppannan Sekar[a,*], Mahendra Mohan Kothottil [b]

[a] Department of Science and Humanities, Anna University – University College of Engineering, Dindigul, 624622, India
[b] Institute for Stem Cell Science and Regenerative Medicine (InStem), Bangalore, India

ARTICLE INFO

Keywords:
Carbazole
Benzothiazole
Mercury ions
Sensor
Protein
Voltammetry

ABSTRACT

The sensor 2-(benzothiazol-2-yl)-1-((9-ethyl-9H-carbazol-6-yl)methylene)hydrazine (**CBT-1**) is successfully synthesized. The sensor **CBT-1** showed selective detection of Hg^{2+} ions in pool of different metal ions through colorimetric and fluorimetric color changes. The sensing mechanism involves Intramolecular charge transfer process between carbazole unit and benzothiazole moiety on interaction with Hg^{2+} ions. The binding nature of **CBT-1** and Hg^{2+} ion is understood with help of varied analytical techniques such as UV–vis, fluorescence, Mass IR spectral analysis and computational studies. The protein binding studies of **CBT-1** and **CBT-1**+$\mathbf{Hg^{2+}}$ ensemble with protein (Bovine Serum Albumin, BSA) is carried out through one- and three-dimensional fluorescence spectral studies. The cyclic voltammetric analysis of the sensor **CBT-1** with distinct metal ions has also been carried out to investigate its potential ability in electrochemical sensing of Hg^{2+} ions.

1. Introduction

In recent years, the development of benzothiazole-based sensors has stimulated the interest in designing fluorescent probes for Hg^{2+} ions owing to the greater affinity of mercury towards sulphur compounds. Especially, the presence of thiazole can possess good molecular binding ability and helps in electronic transitional changes [1,2]. The mercury poisoning paved a huge concern on the conservation of environment and ecology. The mercury poisoning causes acrodynia (pink disease), Hunter – Russell syndrome, Minamata disease, disturbs gastrointestinal system, acute myocardial infarction, coronary heart disease, cardiovascular disease, and renal failure [3,4]. Importantly, the mercury leads neurodegenerative disorders like Alzheimer diseases, Parkinson's syndrome, Menkes (loss of hair and hypotonia in new born baby) and disorder in neuronal transmission, and mental retardation in young children [5–7]. Continuous effort has been taken forward for effective measurement and removal of mercury pollutants from environment. However, these techniques or methods find certain occupational difficulties that lead to ineffective detection or removal of mercury and its substrates from environment [8]. The admissible limit of Hg^{2+} in drinking water followed by US-EPA and WHO is about <0.1 μg/kg body weights per day intake through food, water, skin or other means. [9–11] Whereas, the small molecule based fluorescent sensors are found to be highly utilized for monitoring mercury level in environment and body [12]. These fluorescent sensors have the ability of both selective fluorogenic detection and quantitative estimation of mercury.

Previously, many sensors for mercury ions were reported, for instance, pyrenyl-pyrimidine dye, [13] phenanthrolyl imidazole dye [14], dansyl-rhodamine dye [15], a BODIPY sensor [16], prophyrin derivative [17], dopped graphene quantum dots [18], nanoparitcle based sensors [19], Pyridyl- and benzimidazole-based ruthenium(III) complex [20] etc. However, these sensors find some interference from Cu^{2+}, Fe^{3+} and Cr^{3+} ions and most of these sensors are not either completely soluble in aqueous medium. Recently, the biological monitoring of metal ions is outraged, especially the labeling of metal ions in biomolecules such as protein, DNA etc. are under high concern. For instance, a coumarin based benzimidazole sensor has reported as a selective sensor for Cd^{2+} ions both in solution and protein BSA [21] and naphthalene diamine-based β-diketone sensor [22] was reported as a dual sensing probe and its characteristic binding ability with BSA protein was established. Similarly, a stryl-quinolium sensor was reported for biomolecular interaction with duplex and quadruplex DNA (CT-DNA) through photometric, fluorometric and CD applications [23]. The application of electrochemical stripping metal detection can yield a low detection limit than the fluorescence behavior and are associate with cost effective and ability to perform in in-situ. In the past few

* Corresponding author.
E-mail address: karuppannansekar@gmail.com (S. Karuppannan).

https://doi.org/10.1016/j.jphotochem.2021.113303
Received 6 December 2020; Received in revised form 30 March 2021; Accepted 12 April 2021
Available online 14 April 2021

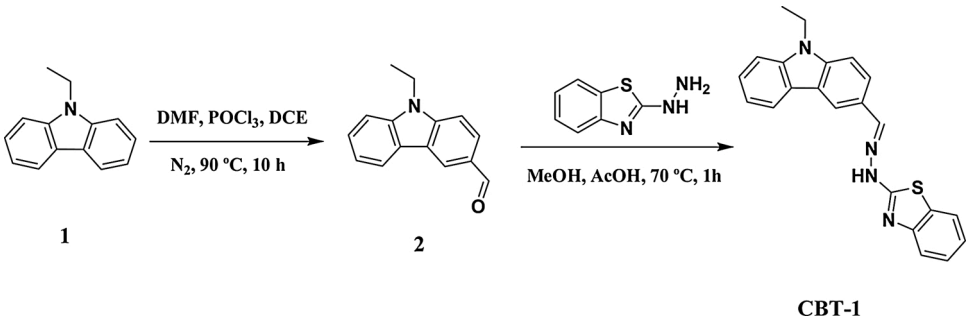

Scheme 1. Synthesis of sensor 2-(benzothiazol-2-yl)-1-((9-ethyl-9H-carbazol-6-yl) methylene)hydrazine (CBT-1).

potential electrochemical sensors were reported, for example, benzil - L-tryptophan Schiff base ligand for fluorescent and electrochemical Zn^{2+} detection, [24] organic nanoparticles of disulfide based receptor [25], a non-fluorescent copper-coumarin complex for detection of biothiols, and the carbazole derivatives are good photo-sensitizer and that are used in DSSCs and OLEDs [26,27]. In this report a novel carbazole–hydrazinobenzothiazole sensor, 2-(benzothiazol-2-yl)-1-((9-ethyl-9H-carbazol-6-yl)methylene)hydrazine **(CBT-1)** for selective detection of Hg^{2+} has been established. The sensor displays *turn-on* green fluorescent emission specifically in presence of Hg^{2+} with low interference from co-ions. This sensor showed a lowest detection limit of about 1.41×10^{-7} M. The biological application of the sensor in protein binding analysis and metal targeting in proteins through one- and three-dimensional fluorescence spectral investigation was also carried out. In addition, the electrochemical behavior of the sensor **CBT-1** was investigated in absence and presence of Hg^{2+}. Thus, this report on fluorescent and electrochemical detection of Hg^{2+} ions, its protein binding studies and targeting might have high impact in specific quantification and biomolecular targeting and labeling applications.

2. Experimental section

2.1. Reagents and instrumentation

The reagents 2-hydrazino benzothiazole, methanol and glacial acetic acid have been purchased from Sigma Aldrich Co. Ltd, India. The spectroscopic solvents dimethyl sulphoxide has been procured from Central Drug House Ltd., India. The other solvents like ethanol, metal salts and Bovine serum albumin BSA are obtained from Sigma Aldrich Co. Ltd., India.

The ^{1}H NMR spectral analyses were carried out with 600 MHz Bruker (Avance) FT-NMR spectrometer and ^{13}C NMR with 125 MHz Bruker (Avance) FT-NMR spectrometer. Molecular mass spectral (ESI-MS) analysis was recorded from positive ion mode – liquid chromatography ion trap mass spectrometer (LCQ Fleet Thermo Fisher Instrument Limited, US). FTIR spectral studies were obtained from Perkin-Elmer spectrometer equipment (version 10.03.09) using KBr pellets. UV–vis spectral analyses were conducted with UV–vis spectrophotometer (ANTECH, Model AN-UV-7000). Fluorescence emission spectral analyses were conducted with aid of Spectrofluorometer (JASCO, Model FP8200). The electrochemical studies have been performed in Cyclic Voltammeter (Vera STAT MC) instrument with sample CBT-1 with 0.1 M $TBAClO_4$ supporting electrolyte in DMSO and Saturated Calomel Electrode (SCE)and Platinum electrode.

2.2. Synthesis of 2-(benzothiazol-2-yl)-1-((9-ethyl-9H-carbazol-6-yl) methylene)hydrazine (CBT-1)

2 g (0.0089 mol) 9-ethyl-9H-carbazolyl-3-carbaldehyde (**2**) [28,29] is dissolved in 20 mL dry methanol. To this solution 1.5 g (0.009 mol) hydrazine benzothiazole is added with two drops of glacial acetic acid. The reaction mixture is then refluxed at 65 °C for 1 h; a grayish white solid precipitate out. The crude product was filtered, washed with EtOH-H_2O mixture, and vacuum dried (Scheme 1). Yield:95 %. ^{1}H NMR (DMSO-d_6, 600 MHz), δ_H (ppm): 12.17 (1H, s), 8.41 (1H, s); 8.32 (1H, s); 8.21 (1H, d, 1.00 Hz); 7.91 (1H, d, 1.01 Hz); 7.77 (1H, d, 1.03 Hz); 7.69 (1H, dd); 7.64 (1H, dd); 7.49 (1H, bd); 7.43 (1H, bd); 7.30 (1H, bd); 7.25 (1H, bd); 7.10 (1H, s); 4.46 (2H, q, 2.15 Hz); 1.33 (3H, t).^{13}C NMR (DMSO-d_6, 125 MHz), δ_C (ppm): 167.34, 140.83, 140.45, 126.65, 126.39, 125.85, 124.29, 122.80, 122.59, 121.96, 121.84, 121.03, 120.36, 119.80, 110.15, 109.94, 37.63, and 14.22. FT-IR (KBr, cm^{-1}) 3434.82, 3185.96, 3062.68, 3015.48, 2974.36, 2874.86, 1617.43, 1577.19, 1476.95, 1445.88, 1371.91, 1330.74, 1297.29, 1270.32, 1234.41, 1193.32, 1118.98, 1018.88, 922.85, 904.19, 883.31, 794.46, 723.39, 741.32, 632.07, 608.18, 561.42, 422.51.Mass (ESI-MS) 371.17 *m/z*. $(M+H)^+$: $(CBT\text{-}1+H)^+$.

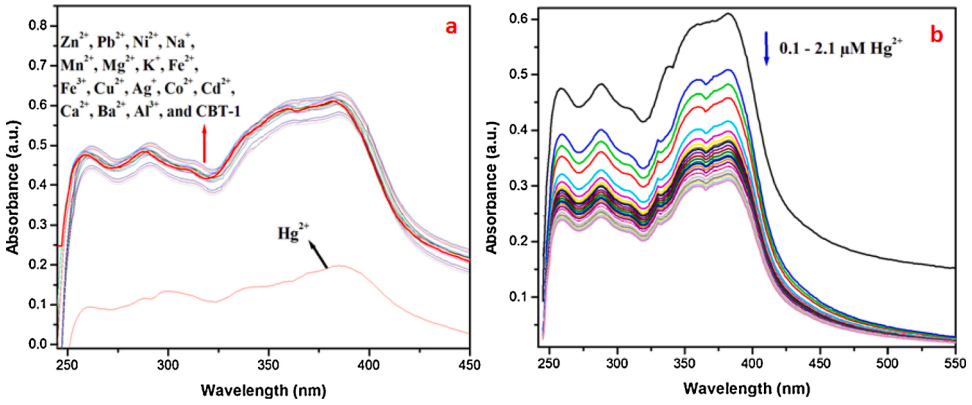

Fig. 1. UV–vis spectrum of probe CBT-1 (1×10^{-6} M, pH 7.5) (a) in the presence of various competitive metal ions (1×10^{-6} M) (b) upon addition of Hg^{2+} (0.1 - 2.1 μM) in DMSO:H_2O (1:9) mixture (λ_{em} =382 nm).

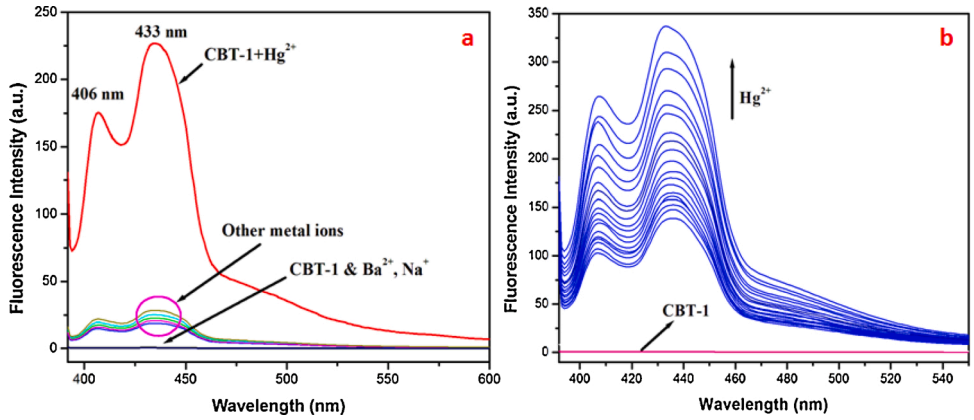

Fig. 2. Fluorescence spectrum of probe CBT-1 (1×10^{-6} M in DMSO: H_2O (1:9), pH 7.5) (a) in the presence of various competitive metal ions (1×10^{-6} M) at λ_{ex} 382 nm, (b) upon addition of (0-2.1 eq) Hg^{2+} λ_{ex} at 382 nm (λ_{em} =433 nm).

3. Result and discussion

3.1. Synthesis and characterization of 2-(benzothiazol-2-yl)-1-((9-ethyl-9H-carbazol-6-yl)methylene)hydrazine (CBT-1)

The sensor **CBT-1** has been successfully synthesized from reaction of 9-ethyl-9H-carbazolyl-3-carbaldehyde (**2**) with 2-hydrazine benzothiazole in methanol and few drops of acetic acid under reflux condition. The formation of **CBT-1** is noted with grayish white solid product. The crude is wash with EtOH-H_2O mixture to remove precursor compounds and vacuum dried (Scheme1).

From ^{1}H NMR, the presence of a singlet peak at 8.41 ppm of imine proton **5** and appearance of new broad and also low intense peak at 12.17 ppm of secondary amine N-H proton indicates the formation of imine product. Further, the presence of aryl proton peaks numbered **7**, **8**, **9** & **10** of benzothiazole unit showed that the hydrazine-benzothiazole is coupled through the carbaldehyde of carbazole forming **CBT-1** sensor and this also confirmed by the characteristic carbon peak in the ^{13}C NMR spectrum (**Fig.S1** and **S2**).

In addition, from the FTIR spectrum (**Fig.S3**) the new appearance of vibrational peak of N—H stretching at 3434 cm^{-1}, C═N stretching band at 1617 cm^{-1} of imine and benzothiazole and the N—H bending frequencies at 1476 cm^{-1} indicated the formation of the ligand **CBT-1**. The formation of sharp peak around the fingerprint regions around 1330 to 1110 cm^{-1} and 900 to 600 cm^{-1} attributed to the C—N stretching of imine and N—H wagging vibrational energies respectively has also indicate the purity of **CBT-1** and the ESI-Mass peak found at 371.17 *m/z* further supports the characteristic evidences (**Fig.S4**).

3.2. UV–vis spectral studies

The absorption spectra of the ligand **CBT-1** showed three peaks at 260 nm, 290 nm and 382 nm in DMSO-H_2O (1:9) medium (Fig.1). The band 260 nm and 290 nm are assigned to the π-π* and the band at 382 nm is assigned to the n-π* electronic transitions of carbazole and hydrazinyl benzothiazole moiety of **CBT-1**. The low intense band at 250 nm–300 nm might be due to solvent effect. From Fig.1**(a)** it is noticed that addition of different metal ion solution say, Zn^{2+}, Pb^{2+}, Ni^{2+}, Na^{+}, K^{+}, Mn^{2+}, Mg^{2+}, Fe^{2+}, Fe^{3+}, Cu^{2+}, Ag^{+}, Co^{2+}, Cd^{2+}, Ca^{2+}, Ba^{2+}, and Al^{3+} (1×10^{-6} M) in DMSO:H_2O (1:9) haven't produce any significant change on the absorption of ligand **CBT-1**. Whereas, the addition of Hg^{2+} to the ligand has greatly quenched the absorption band at 382 nm, this indicates the selectivity of **CBT-1** to Hg^{2+} ions. Also, the larger quenching around 250–300 nm and broad band around 350–420 indicates the Intramolecular charge transfer process is thus involved in sensing of Hg^{2+} ions. This results in donation of electron from imine unit to benzothiazole unit of **CBT-1** through charge transfer effect of carbazole moiety.

In addition, the UV–vis titration study has been carried out. The incremental addition of Hg^{2+} ions to ligand **CBT-1** showed a gradual quenching in absorption band at 382 nm with slight blue shift (Fig.1b), denotes the highly sensitive nature and enhancement of ICT process around 350–420 nm might takes place from carbazole unit to benzothiazole moiety. [30,31] Also, the larger quench around 260 and 290 nm peak and slight quench at 382 nm band insist the interaction of Hg^{2+} to imine nitrogen and sulphur of benzothiazole unit. Further, in solution media the addition of 1 equivalent of Hg^{2+} ions to the **CBT-1** solution showed a color change from colorless to green color under visible light.

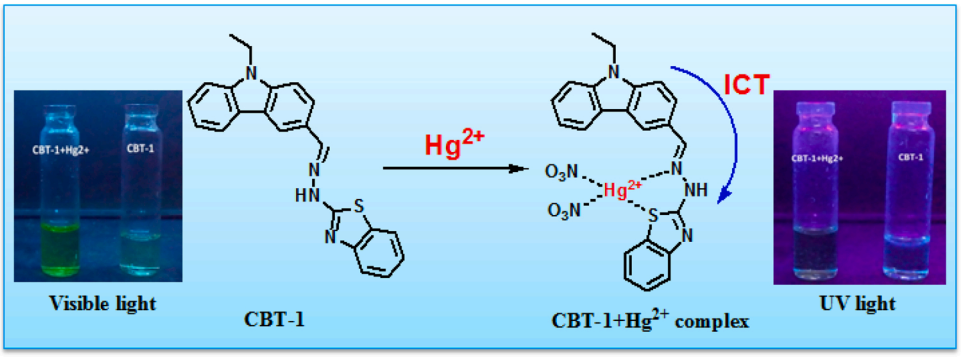

Scheme 2. Proposed sensing mechanism of CBT-1 with Hg^{2+} ion.

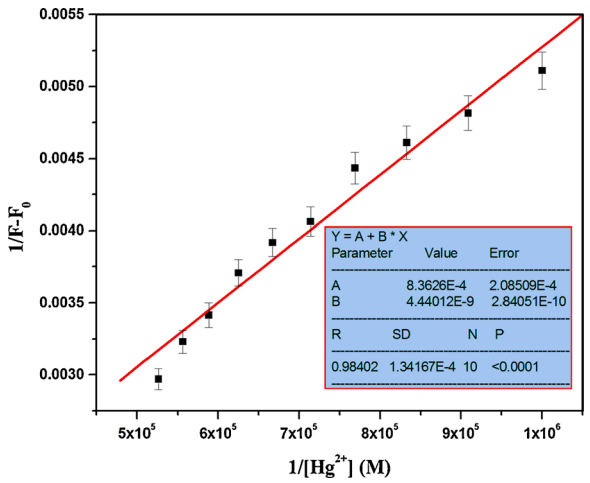

Fig. 3. Benesi-Hildebrand's Plot of CBT-1 with Hg^{2+} at λ_{em} =433 nm (λ_{ex} =382 nm).

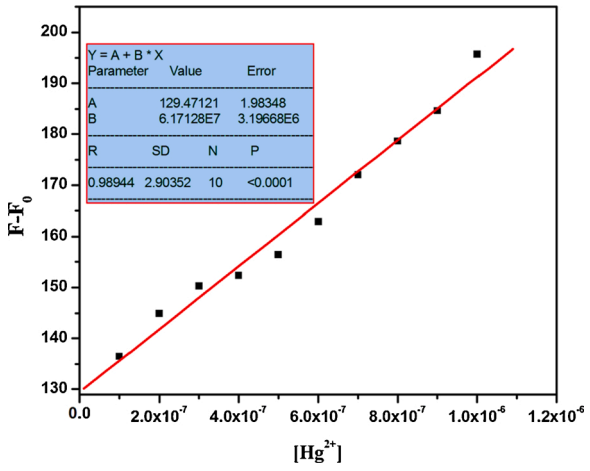

Fig. 4. Linear plots between F-F_0 Vs [Hg^{2+}] at λ_{em} =433 nm (λ_{ex} =382 nm).

3.3. Fluorescence spectral studies

The fluorescence selectivity of the ligand **CBT-1** was further confirmed from emission spectral studies with excitation at 382 nm. The emission spectrum of ligand **CBT-1** showed a low emissive band at 406 and 433 nm, the addition of different metal ions to **CBT-1** is indicated with minimal change emission around 433 nm (Fig.2a). While the addition of 1 equivalent of Hg^{2+} brought about a larger enhancement in fluorescence intensity as shown in Fig.2a, this indicates the selectivity of Hg^{2+} over other metal ions and Intramolecular charge transfer process between carbazole and benzothiazole moiety (Scheme 2). [32]

Similarly, in the titration experiment a gradual raise in emission intensity at 433 nm with respective addition of Hg^{2+} ion solution (Fig.2b). This gradual enhancement of fluorescence showed enhancement of Intramolecular charge transfer process of **CBT-1** on interaction with Hg^{2+} ions. Further from the optical spectral analysis it understood that the involvement of strong Intramolecular charge transfer might be due to the interaction of Hg^{2+} ion with imine nitrogen and benzothiazole sulphur atom. A fluorogenic color change from colorless solution of **CBT-1** to blue color after addition of Hg^{2+} was also observed under UV light. From Job's plot experiment shown in **Fig. S5**, a maximum at 0.5 mole fraction indicates the 1:1 stoichiometric composition was formed, which was further supported with the mass peak at 570.00 *m/z* (CBT-1+Hg^{2+}+H) and 854.42 *m/z* (CBT-1+Hg^{2+}+4NO_3+2Na+2 H) (**Fig.S6**).

The binding constant K_a of the ensemble **CBT-1+Hg^{2+}** complex was found to be 1.88×10^5 M^{-1} (R = 0.98402), calculated from slope of linear plot shown in Fig.3 using Benesi Hildebrand equation (Equation no. **E1,** *see supplementary data*). [33] The lowest detection limit of the CBT-1 for Hg^{2+} ions was calculated to be 1.41×10^{-7} M (R = 0.98944) from slope of the linear plot between F-F_0 and [Hg^{2+}] in the equation **E2** depicted in supplementary data (Fig.4). [34]. In addition, the relative fluorescence quantum yield was also measured using the equation **E3** (*see supplementary data*) with Rhodamine B as standard reference (Φ_r = 0.50 in EtOH) and was found to be 0.0019 (Φ_{CBT-1}) and 0.7918 ($\Phi_{CBT-1+Hg2+}$) in DMSO:H_2O(0.1:0.99, v/v). [35,36]

3.4. Fluorescence stability

The influence of co-existing metal ions on fluorescence of the ensemble **CBT-1+Hg^{2+}** has been studied in DMSO-H_2O (1:9) at 433 nm. The Fig. 5**a** clearly pointing that no absolute changes on fluorescence of ensemble were observed in presence of other metal ions. The pH variation plot shown in Fig. 5**b** reveals on varying the pH of **CBT-1+Hg^{2+}** solution from 2 to 6, the fluorescence intensity was low and gradually approaches the maximum intensity.

While the fluorescence was notably high and stable between the pH 6–10, which suggest that the ligand can be used in physiological conditions and further increasing the pH the fluorescence intensity decrease gradually. The reason might be at acidic condition, the protonation of the nitrogen in the thiazole unit had brought about low emission [37–39] and at the basic pH, the formation of the $Hg(OH)_2$ have caused the less availability of Hg^{2+} ions for interaction. These studies indicate that the ligand and the ensemble emission is quite stable under the influence of interfering metal ions and possibly tend to produce high and stable emission with wide range of pH between 6–10.

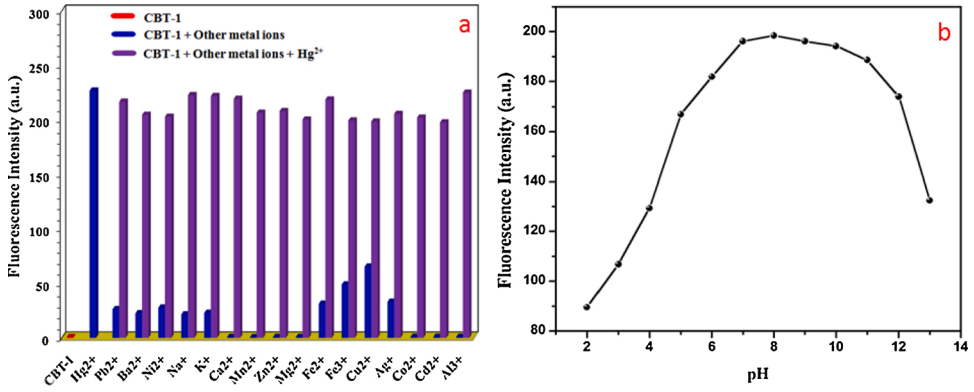

Fig. 5. (a) Fluorescence response of CBT-1 (1×10^{-6} M, pH 7.5) with Hg^{2+} ions in presence of interfering metal ions at λ_{em} =433 nm (λ_{ex} =382 nm), (b) Effect of varying pH range on fluorescent response of CBT-1 towards Hg^{2+} ions at λ_{em} =433 nm (λ_{ex} =382 nm).

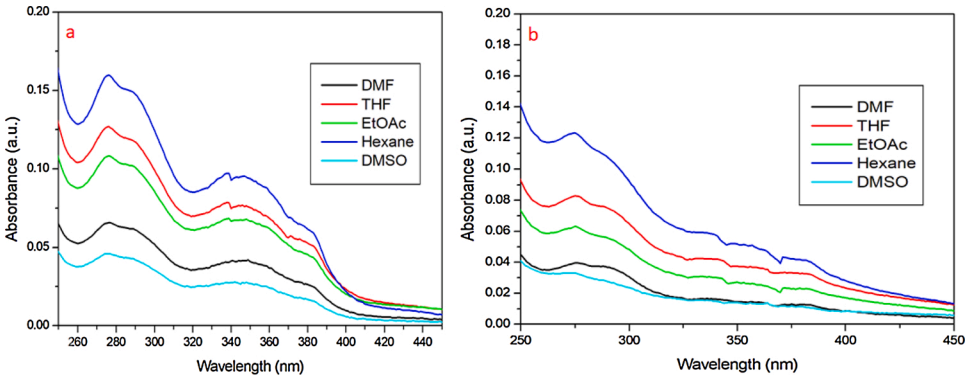

Fig. 6. Polarity effect (a) CBT-1 and (b) CBT-1+Hg^{2+} in pure solvents.

3.5. Binding properties

Further, the mode of binding between ligand **CBT-1** and Hg^{2+} was studied using NMR and FTIR spectra. The ^{1}H NMR titration of the ligand **CBT-1** is studied with addition of Hg^{2+} ions in DMSO-d_6 (**Fig.S7** *see supplementary data*). From the spectra it can be noted that the NH (**6**) proton peak of ligand at δ 12.17 ppm has disappeared upon titration with Hg^{2+} ions, It was also noted that the C–H proton peak (**5**) adjacent to imine group (−HC = N-) shift to 9.02 ppm from 8.41 ppm. These alterations in chemical shift to downfield of protons indicate the strong binding of Hg^{2+} with the imine and tertiary nitrogen atoms. It was also doubted that the imine carbon might also involved in binding, but from the ^{13}C NMR peak of imine 167.34 ppm showed only minimal chemical shift, thus the imine carbon doesn't participate in the binding with Hg^{2+} ion (**Fig.S8** *see supplementary data*).

In addition, the involvement of benzothiazole in binding was also been clearly observed from the chemical shift of proton peaks of **9** and **8** protons of benzothiazole unit from 7.49 & 7.25 ppm–7.53 ppm and got broaden. Also, the doublet of doublet proton peaks of **10** & **7** hydrogen atoms was found to shift downfield from 7.90 ppm & 8.21 ppm to 8.12 ppm & 8.31 ppm and broadened. This indicates that the sulphur atom of thiazole unit involved in the binding with the Hg^{2+} ions and the whole binding mechanism follows HSAB principle.

From the FT-IR spectral titration plot shown in **Fig. S9** (*see supplementary data*), after Hg^{2+} addition, the IR band of N—H stretching frequency at 3434 cm^{-1} of **CBT-1** shifts to 3437 cm^{-1} with increase in

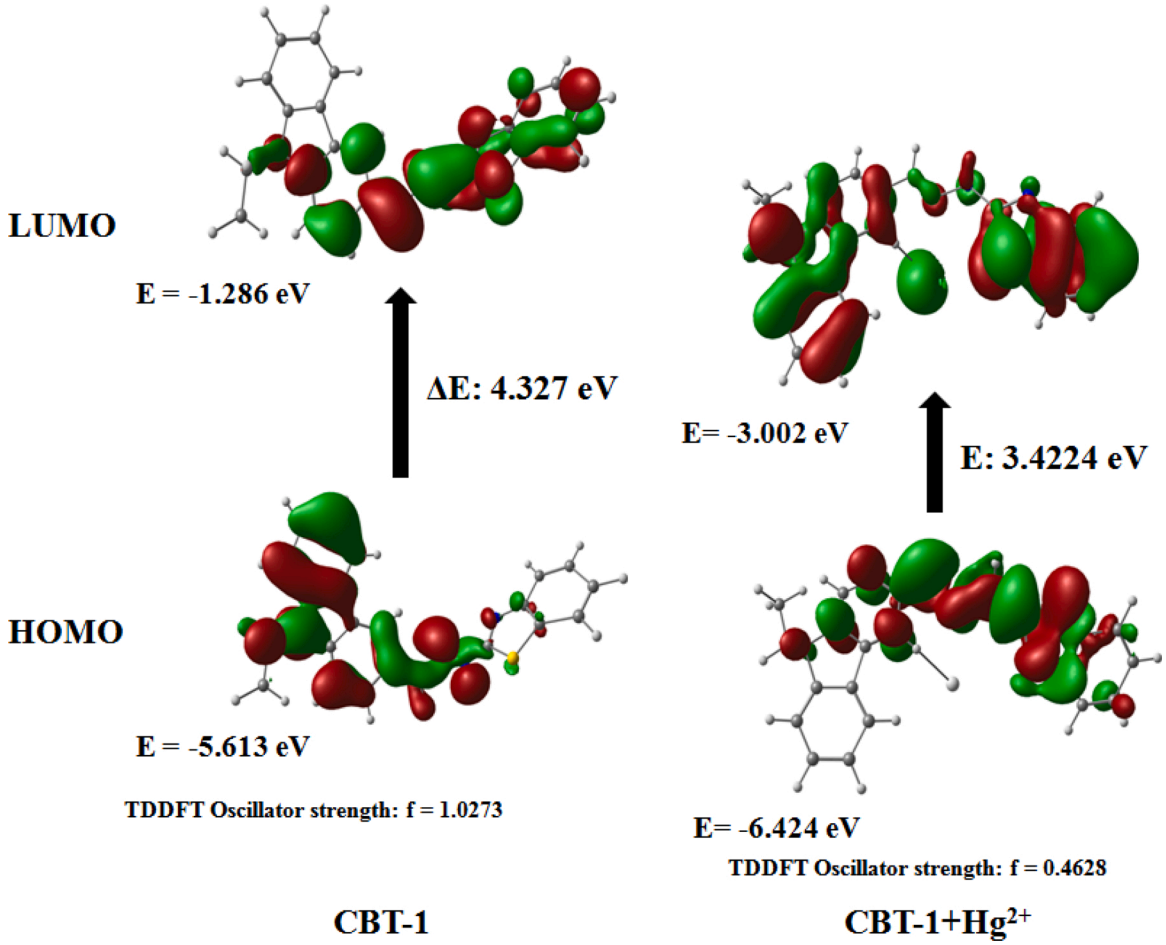

Fig. 7. Frontier Molecular Orbitals of CBT-1 and CBT-1+Hg^{2+}.

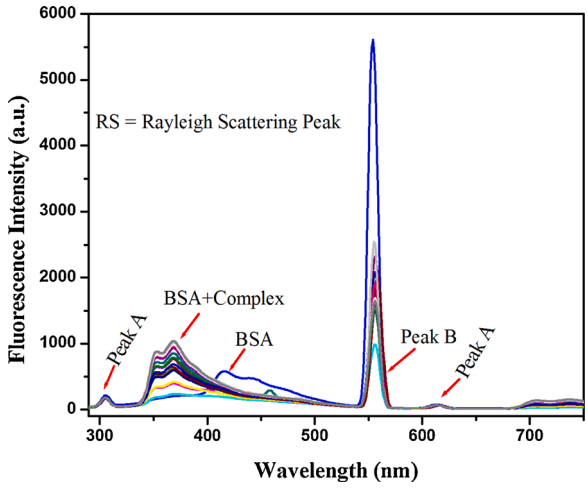

Fig. 8. Fluorescence response of BSA with incremental addition of CBT-1+Hg^{2+} ensemble at λ_{em} =368 nm (λ_{ex} =278 nm).

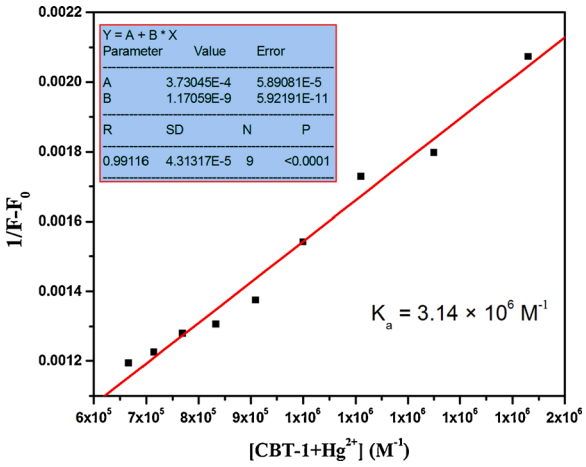

Fig. 9. Binding constant of BSA and CBT-1+Hg^{2+} ensemble at λ_{em} =368 nm (λ_{ex} =278 nm).

absorption. Also, the secondary amine NH bending vibration at 1476 cm^{-1} shifted to 1441 cm^{-1}, and the C = N_{str} of CBT-1 shift from 1617 cm^{-1} to 1597 cm^{-1}. In addition, C-N_{str} and C-S_{str} at 1330 to 1110 cm^{-1} also get alters. This observation reveals that the Hg2+ ion interacts with nitrogen atom of imine and secondary amine as well as the sulphur atom of benzothiazole of **CBT-1**. From the photometric, fluorometric, NMR, Mass, and IR studies of the complex **CBT-1**+$\mathbf{Hg^{2+}}$, the binding mode between ligand **CBT-1** and $\mathbf{Hg^{2+}}$ ion is proposed as depicted in Scheme 2.

3.6. Sensing mechanism

To investigate role of Intramolecular charge transfer mechanism in **CBT-1** sensing Hg^{2+} ions, the UV–vis spectra of **CBT-1** and **CBT-1**+$\mathbf{Hg^{2+}}$ was recorded in pure solvents of different polarity and spectra are shown in Fig. 6. The spectra showed a red shift in lower energy band on increasing polarity of the solvent, similar type of observation was noticed by Chakraborty et al. [40] and Sowmya et al. [41]. For instance, from the Fig. 6a, the lower energy band of **CBT-1** appears at 381 nm in hexane, on increasing the polarity the ligand showed no change in absorption wavelength. However, the lower energy band of **CBT-1**+$\mathbf{Hg^{2+}}$ complex (Fig. 6b) was found at 382 nm in hexane, further increasing the polarity and in the high polar medium DMSO, the absorption band get red shifted to 383 nm. This red shift in absorbance with increasing solvent polarity indicates that the excited state of **CBT-1**+$\mathbf{Hg^{2+}}$ is more polar than the ground state relates to the Intramolecular Charge Transfer process that happens through donation of electron from carbazole to hydrazine benzothiazole unit. [42–44]

In addition, to support the observed photophysical changes of probe **CBT-1** after binding of Hg^{2+} ions and the Intramolecular charge transfer process, the Density functional theory calculations were carried out using Gaussian 09 program. Initially, the geometries of the probe and **CBT-1**+$\mathbf{Hg^{2+}}$ complex were optimized by B3LYP/6−311 G (d,p) and LANL2DZ basis sets respectively, using the optimized geometries IR spectra are generated did not show any negative vibrations signifying the structure is fine (Fig. 7). Further, the TDDFT calculations were carried out with the optimized geometries of **CBT-1** and **CBT-1**+ $\mathbf{Hg^{2+}}$ complex using above said basis sets. The stimulated TDDFT spectra are clearly matching with the observed experimental data. Frontier molecular orbital analysis of **CBT-1** and **CBT-1**+ $\mathbf{Hg^{2+}}$ complex clearly showing that the operation of internal charge transfer mechanism is taken place. In probe HOMO is localized on carbazole unit and LUMO is extend over on the benzothialzole unit, after formation of Hg^{2+} complex thiazole unit with carbazole acts as HOMO and Hg^{2+} behaves as LUMO. It's clearly confirming that the clear disturbance of Internal Charge Transfer (ICT) in probe after appendage of Hg^{2+} ions (Fig. 7).

3.7. Protein binding studies

In significance to the optical sensing behavior of ligand **CBT-1** under physiological condition, it was further subjected to protein binding studies to analysis the biological targeting application of Hg^{2+} ions. The interaction of the fluorescent organic molecules with proteins is of greater interest on valuable account of their biological availability, distribution and transmission. Albumins proteins are most abundant targets in blood that highly contains tryptophan and tyrosine that readily interact with sulphur, nitrogen containing ligand and complexes. Here the **CBT-1** and its complex **CBT-1**+$\mathbf{Hg^{2+}}$ has been analyzed for the better understanding of their biological potential through interaction with protein samples. [45,46]

The Fig.8 and **S10** is showing the interaction of BSA (1×10^{-5} M) and **CBT-1**+$\mathbf{Hg^{2+}}$ ensemble (1×10^{-5} M), from these figures it is observed that after addition of **CBT-1**+$\mathbf{Hg^{2+}}$ ensemble the emission band of BSA got blue shifted to 368 nm from 415 nm and gradually increase in intensity when excited at 278 nm. This characteristic changes in band revealed the strong interaction of **CBT-1**+$\mathbf{Hg^{2+}}$ with amino-acids, tryptophan and tyrosine. This intrinsic fluorescence spectral change of the tryptophan and the tyrosine due to interaction of **CBT-1** complex has depicted the conformational changes lead through micro-environment changes around these two residues. The protein binding constant has been determined using Benesi-Hildebrand plot (Fig. 9) and equation (**E1**) (*see supplementary data*). The binding constant calculated from using the slope in the B–H equation found to be $K_{BSA+(CBT-1+Hg2+)} = 3.14 \times 10^6$ M^{-1} (R = 0.99116). The polarity effect was also considered, from the fluorescence spectra as shown in **Fig. S11** was observed that change in polarity ranging from acetone, ethyl acetate, DCM, THF, DMF, DMSO with as medium does not apparently affect the fluorescence of the BSA + CBT-1+Hg^{2+} ensemble (**Fig. S11** *see supplementary data*).

3.8. Three-dimensional fluorescence studies of BSA

Three-dimensional fluorescence spectral studies have been carried out for understanding the conformational and microenvironmental changes of tryptophan and tyrosine in the presence of sensor **CBT-1** and its Hg^{2+} complex. The 3D spectrum of BSA in **Fig. S12** (*see supplementary data*) has five peaks, in which the peak A, B and C are the first, second and third order Rayleigh scattering peak respectively. [47] The peak **1** represents the emission band of the polypeptide backbone of the BSA and the peak **2** is the intrinsic fluorescence emission band of tryptophan

Table 1
Redox Potentials and Current of CBT-1 in presence and absence of Hg^{2+} ions.

	E_{pa} (V)	E_{pc} (V)	I_{pa} (A)	I_{pc} (A)	ΔE_p (V)	I_{pa}/I_{pc}
CBT-1	−0.63488	−1.23327	1.72×10^{-7}	-3.60×10^{-6}	0.59839	−0.04778
	0.56097	0.79468	2.03×10^{-6}	3.15×10^{-7}	0.23371	6.4444
CBT-1+Hg^{2+}	−0.10551	0.1052	3.30×10^{-6}	-1.85×10^{-6}	−0.21071	−1.783784
	0.77229	0.86399	7.36×10^{-6}	1.62×10^{-6}	−0.0917	4.54321

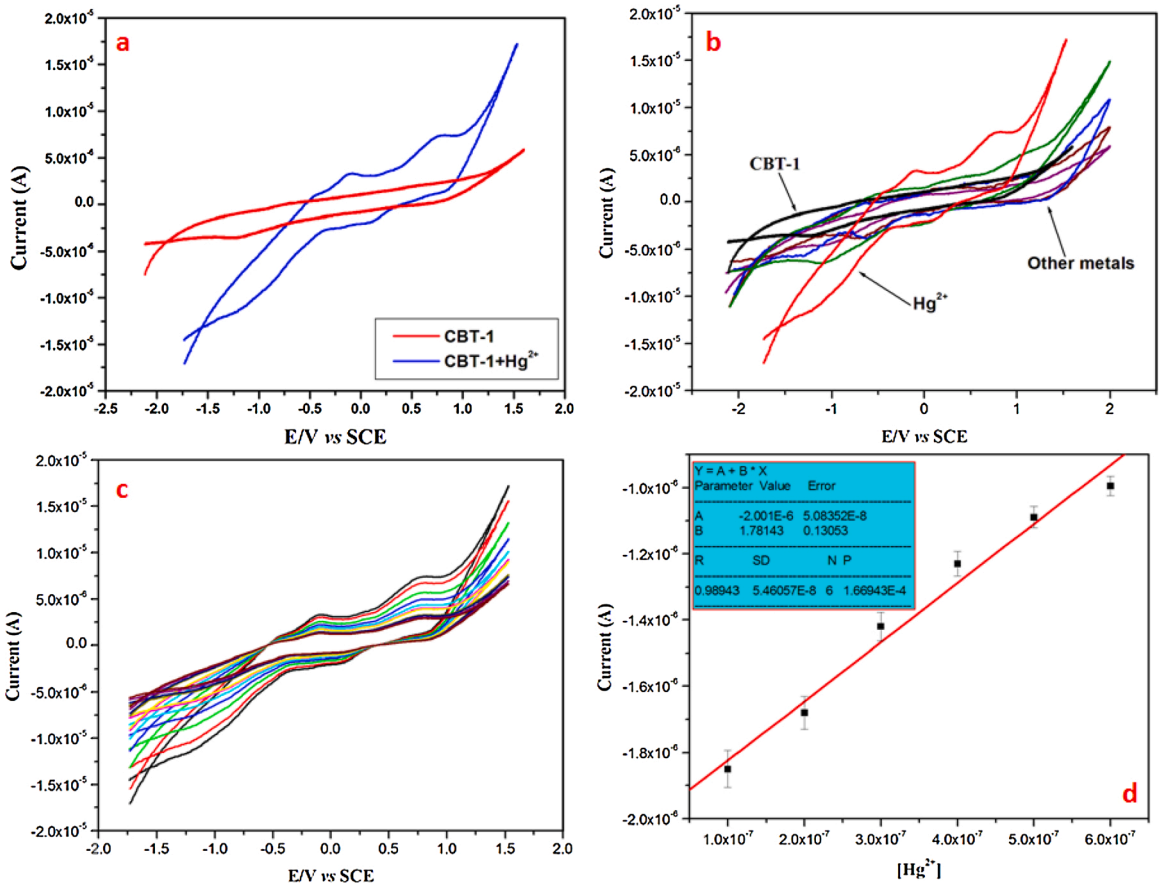

Fig. 10. Cyclic voltammograms of (a) CBT-1 with and without Hg^{2+} ion, (b) CBT-1 with metal ions, (c) CBT-1 titration with Hg^{2+} ions, (d) Linear Plot Current Vs [Hg^{2+}] in 0.1 M $TBAClO_4$/DMSO Vs SCE.

and tyrosine (**Fig. S13** *see supplementary data*). The binding of ligand **CBT-1** and detection of Hg^{2+} in protein BSA is to understand the biological activity of ligand in targeting the analytes in subcellular organelles, lysosomes, and to derive the ability of ligand in diagnosing human body and docking purposes.

When the native BSA is treated with complex **CBT-1+Hg^{2+}** the 3D fluorescence spectra interestingly have showed greater magnitude of quenching in peak **1** and **2** and formed a single adduct broad band at 370 nm (at λ_{ex} 270) (**Fig.S14** *see supplementary data*).This conformational change of polypeptide backbone and microenvironment of the tryptophan and tyrosine has indicated the strong interaction of the complex **CBT-1+Hg^{2+}** with BSA (**Fig.S15** *see supplementary data*). The Stokes shift of the complex adduct of BSA is found to be lower than peak **1** and peak **2** the shifts might be due the hydrophobicity nature around the tryptophan and tyrosine and polypeptide backbone (Table 1).

From the **Fig. S16** the 3D spectra and 2D contour spectra of BSA treated with **CBT-1** (**Fig.S17** *see supplementary data*) has showed a relative low fluorescence compared to BSA with **CBT-1+Hg^{2+}** Complex and native BSA. Also, from the upper view and the contour plot of the BSA, BSA treated with complex and **CBT-1** it was observed that the depth of the 2D contour was being reduced respectively. This indicate the interaction of the **CBT-1** ligand in complex was much contributed for interaction of polypeptide, tryptophan, tyrosine in BSA through hydrazino – nitrogen and sulphur and nitrogen benzothiazole which indicate the ligand and its Hg^{2+} complex might be used for biomolecular targeting in proteins.

3.9. Electrochemical application

Since, the **CBT-1** act as a good sensor for Hg^{2+} revealed from the above experiments and considering the electron rich conjugated molecular structure and charge transfer effect of the complex system, the ligand can also perform as an electrochemical sensor. For this the voltametric response of sensor **CBT-1** was tested in absence and presence of Hg^{2+} ion in tetrabutyl ammonium perchlorate solution (0.1 M $TBAClO_4$) as supporting electrolyte in DMSO solution. [48–50] During sweep scan of free **CBT-1** in solution, the sensor produce a reversible potential sweep with low potential and low current yield (Fig. 10a). The anodic scan of the **CBT-1** showed two oxidation potential, first one at $E_{1/2}$ = -0.63448 V [$\Delta E_p = 0.59839$ V, I_{pa}/I_{pc} =-0.04778] and second one at $E_{1/2} = 0.56097$ V [$\Delta E_p = 0.23371$ V, $I_{pa}/I_{pc} = 6.4444$], this two-oxidation potential indicates the Intramolecular Charge Transfer

process due to electron charge transfer. After addition of 1 equivalent of Hg^{2+} solution to the cell, the first oxidation potential of the **CBT-1** has found to shift to higher potential $E_{1/2}$ = -0.10551 V [ΔE_p = -0.21071 V, I_{pa}/I_{pc} = -1.783784] and the second oxidation potential moved to $E_{1/2}$ = 0.77229 V [ΔE_p = -0.0917 V, I_{pa}/I_{pc} = 4.54321] (Fig.10a). It can be noticed that the oxidation potential increase after addition of Hg^{2+} ions (Table 1), it might be due the chelation process electron transfer from the lone pairs of imine nitrogen and sulphur that indicates the oxidation of **CBT-1** with two electron system and also supports the formation of **CBT-1**+$\mathbf{Hg^{2+}}$ complex. [51] A comparison have been made based on previously reported Hg^{2+} ionic sensors and present work (**Table S2**)

The competitive cyclic voltagram of **CBT-1** with different metal ions showed a selective recognition of Hg^{2+} as depicted in Fig. 10**b** and the incremental addition of Hg^{2+} ion showed a gradual drop and increase in respective redox potential (Fig. 10c), which also states that the **CBT-1** is highly sensitive to electrochemical changes specifically in presence of Hg^{2+} ions. The limit of detection obtained from cyclic voltagram is 9.2×10^{-8} M (Fig.10d).

3.10. Comparison of optoelectrochemical and biological property of CBT-1 sensor

From the experimental analyses, it is found that the **CBT-1** is excellent optical sensor for Hg^{2+} ions with lowest detection limit of 1.41×10^{-7} M and strong binding nature. However, in the electrochemical behavior the ligand **CBT-1** showed more lowest detection level 9.2×10^{-8} M, which indicates that electrochemical sensing property is superior to fluorescence sensing of **CBT-1**. However, in both cases, the sensor is highly selective towards Hg^{2+} and thus follows the Intramolecular charge transfer mechanism. In addition, to this the sensor **CBT-1** is also a good biological targeting agent, which was evident from strong protein binding nature.

3.11. Conclusion

The sensor **CBT-1** has been synthesized successfully through simple method. This sensor has potential ability in selectively detecting Hg^{2+} through turn on green emission. The sensor **CBT-1** established high emission specifically in presence of Hg^{2+} ions over 200 a.u. in intensity at 433 nm with excitation at 382 nm through Intramolecular Charge Transfer process. This sensor **CBT-1** can able to detect the Hg^{2+} content in aqueous media to about 1.41×10^{-7} M (R = 0.98944). The fluorescence emission of the ligand with Hg^{2+} is not interfered by the presence of other co-existing metal ions and quiet photostable between 6–11 pH values of the solution. The complexation between ligand **CBT-1** and Hg^{2+} through coordination of nitrogen atoms of hydrazine unit and the sulphur atom of benzothiazole unit has been figured out using ^{1}H NMR, Mass and IR titration studies. The application of ligand **CBT-1** and its Hg^{2+} complex in protein binding using simple and 3D fluorescence studies with BSA has indicated the portability of the sensor and its complex in targeting Hg^{2+} in cells and subcellular organelles. The shift to higher oxidation potential of ligand **CBT-1** in presence of Hg^{2+} indicates the possible feasibility of electrochemical process due the chelation effect. The lowest detection limit found using electrochemical method is 9.2×10^{-8} M.

Declaration of Competing Interest

On behalf of all the authors of this manuscript, I declare that the authors have **No Conflict of Interest** in publishing this work in your journal.

Acknowledgements

C. Denzil Britto is thankful to DST-SERB, New Delhi, India for project fellowship and K. Sekar is grateful Department of Science and Technology - Science and Engineering Research Board (DST-SERB), New Delhi, India for financially supporting the project (Grant No. SB/FT/CS-062/2013).

Appendix A. Supplementary data

Supplementary material related to this article can be found, in the online version, at doi:https://doi.org/10.1016/j.jphotochem.2021.113303.

References

[1] B. Gu, L. Huang, W. Su, X. Duan, H. Li, S. Yao, A benzothiazole-based fluorescent probe for distinguishing and bioimaging of Hg2+ and Cu2+, Anal. Chim. Acta 954 (2017) 97–104.
[2] A. Singh, A. Singh, N. Singh, D.O. Jang, Selective detection of Hg(II) with benzothiazole-based fluorescent organic cation and the resultant complex as a ratiometric sensor for bromide in water, Tetrahedron 72 (24) (2016) 3535–3541.
[3] M. Tian, L. Liu, Y. Li, R. Hu, T. Liu, H. Liu, S. Wanga, Y. Li, An unusual OFF–ON fluorescence sensor for detecting mercury ions in aqueous media and living cells, Chem. Commun. (Camb.) 50 (2014) 2055–2057.
[4] A. Robert, Y. Liu, M. Nguyen, B. Meunier, Regulation of copper and iron homeostasis by metal chelators: a possible chemotherapy for Alzheimer's disease, Acc. Chem. Res. 48 (2015) 1332–1339.
[5] K.P. Carter, A.M. Young, A.E. Palmer, Fluorescent sensors for measuring metal ions in living systems, Chem. Rev. 114 (2014) 4564–4601.
[6] A.A. Belaidi, A.I. Bush, Iron neurochemistry in Alzheimer's disease and Parkinson's disease: targets for therapeutics, J. Neurochem. 139 (2016) 179–197.
[7] S. Bayindir, A Simple Rhodanine-Based Fluorescent Sensor for Mercury and Copper: the recognition of Hg2+ in aqueous solution, and Hg2+/Cu2+ in organic solvent, J. Photochem. Photobiol. A: Chem. 372 (2019) 235–244.
[8] J. Sujung, T. Ponnaboina, N.N. Lok, S. Junho, L. Hyunsook, I.L. Wan, L. Keun-Hyeung, Highly sensitive ratiometric fluorescent chemosensor for silver ion and silver nanoparticles in aqueous solution, Org. Lett. 14 (18) (2012) 4746–4749.
[9] Mercury Update: Impact on Fish Advisories, EPA Fact Sheet EPA- 823–S2_01-011, EPA, Office of Water, Washington, DC, 2001.
[10] https://clu-in.org/download/contaminantfocus/mercury/Mercury-CAfs.pdf.
[11] https://www.who.int/water_sanitation_health/dwq/chemicals/mercuryfinal.pdf.
[12] V. Raju, R. Selva Kumar, S.K. Ashok Kumar, G. Madhu, S. Bothra, S.K. Sahoo, A ninhydrin–thiosemicarbazone based highly selective and sensitive chromogenic sensor for Hg2+ and F- ions, J. Chem. Sci. Bangalore (Bangalore) 132 (2020) 89.
[13] W. Jiena, M. Qunbo, L. Qidan, F. Quli, H. Wei, A new colorimetric and fluorescent ratiometric sensor for Hg2+ based on 4-pyren-1-yl-pyrimidine, Tetrahedron 68 (2012) 3129–3134.
[14] B. Gua, L. Huang, N. Mi, P. Yin, Y. Zhang, X. Tu, X. Luo, S. Luo, S. Yao, An ESIPT-based fluorescent probe for highly selective and ratiometric detection of mercury (II) in solution and in cells, Analyst 140 (8) (2015) 2778–2784.
[15] Y. Shizhuang, S. Wei, W. Enju, A dansyl-rhodamine based fluorescent probe for detection of Hg2+ and Cu2+, Acta Chim. Slov. 64 (2017) 638–643.
[16] Z. Baocheng, Q. Siyao, C. Bo, H. Yifeng, A new BODIPY-based fluorescent "turn-on" probe for highly selective and rapid detection of mercury ions, Tetrahedron Lett. 59 (2018) 4359–4363.
[17] Y. Yang, J. Jiang, G. Shen, R. Yu, An optical sensor for mercury ion based on the fluorescence quenching of tetra(p-dimethylaminophenyl)porphyrin, Anal. Chim. Acta 636 (2009) 83–88.
[18] Z. Liu, Z. Mo, X. Niu, X. Yang, Y. Jiang, P. Zhao, N. Liu, R. Guo, Highly sensitive fluorescence sensor for mercury(II) based on boron- and nitrogen-co-doped graphene quantum dots, J. Colloid Interface Sci. 566 (2020) 357–368.
[19] M. Zannotti, V. Vicomandi, A. Rossi, M. Minicucci, S. Ferraro, L. Petetta, R. Giovannetti, Tuning of hydrogen peroxide etching during the synthesis of silver nanoparticles. An application of triangular nanoplates as Plasmon sensors for Hg2+ in aqueous solution, J. Mol. Liq. 309 (2020), 113238.
[20] H. Sharma, H.J. Guadalupe, J. Narayanan, H. Hofeld, T. Pandiyan, N. Singh, Pyridyl- and benzimidazole-based ruthenium(III) complex for selective chloride recognition through fluorescence spectroscopy, Anal. Methods 5 (2013) 3880–3887.
[21] S. Zehra, R.A. Khan, A. Alsalme, S. Tabassum, Coumarin derived "Turn on" fluorescent sensor for selective detection of cadmium (II) ion: spectroscopic studies and validation of sensing mechanism by DFT calculations, J Fluores 29 (2019) 1029–1037.
[22] G. Tamil Selvan, C. Varadaraju, R. Tamil Selvan, I.V.M.V. Enoch, P.M. Selvakumar, On/Off fluorescent chemosensor for selective detection of divalent Iron and copper ions: molecular logic operation and protein binding, ACS Omega 3 (2018) 7985–7992.
[23] A.K. Das, H. Ihmels, S. Kölsch, Diphenylaminostyryl-substituted quinolizinium derivatives as fluorescent light-up probes for duplex and quadruplex DNA, Photochem. Photobiol. Sci. 18 (2019) 1373–1381.
[24] K. Dutta, R.C. Deka, D.K. Das, A new fluorescent and electrochemical Zn2+ ion sensor based on Schiff base derived from benzil and L-tryptophan, Spectrochimica Acta Part A 124 (2014) 124–129.

[25] J. Singh, C.A. Huerta-Aguilar, H. Singh, T. Pandiyan, N. Singh, Voltammetric Simultaneous Determination of Cu2+, Cd2+ and Pb2+ in Full Aqueous Medium Using Organic Nanoparticles of Disulfide Based Receptor, Electroanalysis 27 (2015) 2544–2551.
[26] N. Duvva, R.K. Kanaparthi, J. Kandhadi, G. Marotta, P. Salvatori, F.D. Angelis, L. Giribabu, Carbazole-based sensitizers for potential application to dye sensitized solar cells, J. Chem. Sci. Bangalore (Bangalore) 127 (2015) 383–394.
[27] T.Y. Wu, M.H. Tsao, S.G. Su, H.P. Wang, Y.C. Lin, F.L. Chen, C.W. Chang, I.W. Sun, Synthesis, Characterization and Photovoltaic Properties of Di-Anchoring Organic Dyes, J. Braz. Chem. Soc. 22 (4) (2011) 780–789.
[28] C. Denzil Britto, K. Sekar, K.M. Vengaian, G. Sivaraman, S. Singaravadivel, Carbazole–azine based fluorescence 'off–on' sensor for selective detection of Cu2+ and its live cell imaging, Luminescence 32 (7) (2017) 1354–1360.
[29] C. Denzil Britto, K. Sekar, K.M. Vengaian, G. Sivaraman, S. Singaravadivel, A fluorescent turn-on carbazole-rhodanine based sensor for detection of Ag+ ions and application in Ag+ ions imaging in cancer cells, J. Fluoresc. 29 (2019) 75–89.
[30] S. Goswami, S. Paul, A. Manna, Carbazole based hemicyanine dye for both "naked eye" and 'NIR' fluorescence detection of CN− in aqueous solution: from molecules to low cost devices (TLC plate sticks), Dalton Trans. 42 (2013) 10682–10686.
[31] Q. Zou, F. Tao, H. Wu, W.W. Yu, T. Li, Y. Cui, A new carbazole-based colorimetric and fluorescent sensor with aggregation induced emission for detection of cyanide anion, Dye. Pigment. 164 (2019) 165–173.
[32] L. Yang, W. Zhu, M. Fang, Q. Zhang, L. Cun, A new carbazole-based Schiff-base as fluorescent chemosensor for selective detection of Fe3+ and Cu2+, Spectrochimica Acta Part A109 (2013) 186–192.
[33] Y. Li, J. Wu, X. Jin, J. Wang, S. Han, W. Wu, J. Xu, W. Liu, X. Yao, Y. Tang, A bimodal multianalyte simple molecule chemosensor for Mg2+, Zn2+, and Co2+, Dalton Trans. 43 (2014) 1881–1887.
[34] M. Ahumada, E. Lissi, A.M. Montagut, F.V. Henríquez, N.L. Pacioni, E.I. Alarcon, Association models for binding of molecules to nanostructures, Analyst 142 (2017) 2067–2089.
[35] A.T.R. Williams, S.A. Winfield, J.N. Miller, Relative fluorescence quantum yields using a computer controlled luminescence spectrometer, Analyst 108 (1983) 1067–1071.
[36] A.M. Brouwer, Standards for photoluminescence quantum yield measurements in solution (IUPAC Technical Report), Pure Appl. Chem. 83 (2011) 2213–2228.
[37] S. Mondal, R. Raza, K. Ghosh, Cholesterol linked benzothiazole: a versatile gelator for detection of picric acid and metal ions such as Ag+, Hg2+, Fe3+ and Al3+ under different conditions, New J. Chem. 43 (2019) 10509–10516.
[38] R. Benassi, R. Grandi, U.M. Pagnoni, F. Tadde, Study of the Effect of N-Protonation and N-Methylation on the' H and "C Chemical Shifts of the Six-Membered Ring in Benzazoles and 2-Substituted N,N-Dimethylamino Derivatives', Magn. Reson. Chem. 24 (1986) 415–420.
[39] I. Petkov, T. Deligeorgiev, I. Timtcheva, Effect of the medium acidity on the photophysical characteristics of some 2-aryl- and 2-hetaryl-benzothiazoles, Dye. Pigment. 35 (1997) 171–181.
[40] A. Chakraborty, S. Kar, N. Guchhait, Secondary amino group as charge donor for the excited state intramolecular charge transfer reaction in trans-3-(4-monomethylamino-phenyl)-acrylic acid: spectroscopic measurement and theoretical calculations, J. Photochem. Photobiol. A: Chem. 181 (2006) 246–256.
[41] M. Sowmiya, Amit K. Tiwari, Sonu, Subit K. Saha, Study on intramolecular charge transfer fluorescence properties of trans-4-[4 -(N,N -dimethylamino)styryl] pyridine: effect of solvent and pH, J. Photochem. Photobiol. A: Chem. 218 (2011) 76–86.
[42] S. Bruni, E. Cariati, F. Cariati, F.A. Porta, S. Quici, D. Roberto, Determination of the quadratic hyperpolarizability of trans-4-[4-(dimethylamino)styryl]pyridine and 5-dimethylamino-1,10-phenanthroline from solvatochromism of absorption and fluorescence spectra: a comparison with the electric-field-induced second-harmonic generation technique, Spectrochim. Acta A. 57 (2001) 1417–1426.
[43] M.J. Kamlet, J.-L.M. Abboud, M.H. Abraham, R.W. Taft, Linear solvation energy relationships. 23. A comprehensive collection of the solvatochromic parameters, pi*, alpha, and. beta., and some methods for simplifying the generalized solvatochromic equation, J. Org. Chem. 48 (1983) 2877–2887.
[44] T. Kobayashi, M. Futakami, O. Kajimoto, The charge-transfer state of 4-dimethy-lamino-3,5-dimethylbenzonitrile studied in a free jet, Chem. Phys. Lett. 141 (1987) 450–454.
[45] X. Long, Y.F. Zeng, Y. Liu, Y. Liu, T. Li, L. Liao, Y. Guo, Synthesis of novel genistein amino acid derivatives and investigation on their interactions with bovine serum albumin by spectroscopy and molecular docking, RSC Adv. 8 (2018) 31201–31212.
[46] G. Kalaiarasi, S. Dharani, V.M. Lynch, R. Prabhakaran, Para metallation of 3-acetyl-chromen-2-one Schiff bases in tetranuclear palladacycles: focus on their biomolecular interaction and in vitro cytotoxicity, Dalton Trans. 48 (2019) 12496–12511.
[47] N. Manjubaashini, M.P. Kesavan, J. Rajesh, T.D. Thangadurai, Multispectroscopic and bioimaging approach for the interaction of rhodamine 6G capped gold nanoparticles with bovine serum albumin, J. Photochem. Photobiol. B 183 (2018) 374–384.
[48] N. Bhuvanesh, S. Suresh, K. Velmurugana, A. Thamilselvan, R. Nandhakumar, Quinoline based probes: large blue shifted fluorescent and electrochemical sensing of cerium ion and its biological applications, J. Photochem. Photobiol. A: Chem. 386 (2020), 112103.
[49] C. Kar, G. Das, A retrievable fluorescence "TURN ON" sensor for sulfide anions, J. Photochem. Photobiol. A: Chem. 251 (2013) 128–133.
[50] S.K. Atasen, Y. Alcay, O. Yavuz, B. Yuce, I. Yilmaz, Beryllium ion sensing through the ion pair formation between the electrochemically reduced ferrocenyl naphthoquinone radicals and Be2+ ions, J. Chem. Sci. 131 (2019) 41.
[51] J. Singh, C.A. Huerta-Aguilar, H. Singh, T. Pandiyan, N. Singh, Voltammetric Simultaneous Determination of Cu2+, Cd2+ and Pb2+ in Full Aqueous Medium Using Organic Nanoparticles of Disulfide Based Receptor, Electroanalysis 27 (2015) 2544–2551.